Hindawi
Nanomaterials and Nanotechnology
Volume 2023, Article ID 9980479, 11 pages
https://doi.org/10.1155/2023/9980479

Research Article

Mulberry Juice-Derived Carbon Quantum Dots as a Cu^{2+} Ion Sensor: Investigating the Influence of Fruit Ripeness on the Optical Properties

Chiayee Salih Ajaj and Diyar Sadiq

Centre for Material Science and Nanotechnology (CMSN), Department of Physics, Faculty of Science, University of Zakho, Zakho, Kurdistan Region, Iraq

Correspondence should be addressed to Chiayee Salih Ajaj; chiayee.ajaj@uoz.edu.krd

Received 6 July 2023; Revised 5 September 2023; Accepted 7 September 2023; Published 20 September 2023

Academic Editor: Raphael Schneider

This study synthesized carbon quantum dots (CQDs) with green photoluminescence through a hydrothermal method that utilized mulberry juice as the carbon source. The influence of fruit ripeness on the physical and chemical properties, focusing on the fluorescence spectra, has been explored. Fourier-transform infrared spectroscopy (FT-IR) and energy dispersive X-ray analysis (EDX) showed that there were oxygen-containing groups, and X-ray diffraction (XRD) showed that the carbon quantum dots (CQDs) were graphitic. The results revealed that the CQDs had an average size of around 7.4 nm and 9.7 nm for unripe and ripe mulberry juice, respectively. These CQDs emitted green light at 500 nm and 510 nm in unripe and ripe mulberry juice, respectively, when excited at a wavelength of 400 nm. The prepared CQDs exhibited excitation-dependent photoluminescence (PL) emission behavior, demonstrating their dependence on the excitation light. The impact of fruit ripeness on optical properties was explored by examining fluorescent spectra from different fruits (including tomato and blackberry), demonstrating comparable behaviors observed in mulberry fruit. In addition, the prepared CQDs were utilized as a fluorescent sensor with high specificity to detect Cu^{2+} ions. The detection limit (DL) for this sensor was determined to be 0.2687 μM, and the limit of qualification (LOQ) is 0.814 μM. The linear range for detection lies between 0.1 and 1 μM. The selectivity of the CQDs towards Cu^{2+} ions was confirmed by recording the PL response for Cu^{2+} ions compared to the weak response of other metal ions. According to these results, the CQDs can be applied in various cellular imaging and biology applications, bio-sensing, optoelectronics, and sensors.

1. Introduction

Carbon quantum dots (CQDs) are a class of quantum dots (zero-dimensional nanostructures) that have exclusive properties, consisting of quantum energy levels and excellent optical and electrical properties [1]. The unique characteristics of CQDs include low toxicity, good biocompatibility [2], high water solubility, excellent optical properties, catalytic properties, electrical conductivity, high stability, and easy functionalization that are responsible for their utility in a wide range of applications such as bio-imaging [3], cellular imaging [4], metal sensing [5], drug delivery [6], energy storage [7], optoelectronics [8], sensors [9], light-emitting diode (LED) [10], and antibacterial and tissue engineering [11–17]. Though there has been fast growth in the area of CQDs, their synthesis is pretty challenging due to difficult reaction conditions, damaging starting materials, and steps in surface passivation [11].

To date, the synthesis of CQD has been carried out using natural and renewable green materials. These sources are used to create fluorescent CQDs. The dopant particle size, the dopant's desire, the impact of the passivating agent, pH [5], time, temperature [18], and the nature of the solvent are critical in affecting how the CQDs behave fluorescently. When electron-rich heteroatoms such as nitrogen, boron, and sulfur are doped on the surface of the CQDs, their capacity to fluoresce and their catalytic behaviors are considerably modulated [14]. Moreover, the created CQDs can also be used as efficient fluorescent probes for sensing, catalysis, and biological applications [19, 20].

Nowadays, because they are cheap, abundant, easy to find, and environmentally beneficial, CQD precursors made of green natural materials are becoming increasingly attractive as carbon sources [21]. CDs are a class of quantum dots that can be created from several carbon-based precursors. Numerous studies have demonstrated CQDs with carbon sources from fruit-derived sources, including *Carica papaya* [22], tomato [23], pear, avocado, kiwi [24], tapioca [25, 26], lemon, from perennial grass such as sugarcane [27, 28], and oranges such as satang honey, lime, mandarin, and sweet orange [21]. The techniques for creating CQDs that are most frequently utilized are chemical oxidation, ultrasonic synthesis, hydrothermal synthesis, solvothermal synthesis, microwave synthesis, and laser ablation. Among them, the hydrothermal technique is the most facile approach to the green process because it uses a soft chemical pathway and a one-step synthesis which makes it inexpensive, simple, and affordable and has mild reaction conditions and is environmentally benign. It produces CQDs with uniform particle sizes, making them great candidates for use in many applications. However, despite the extensive effort put into the green synthesis of CQDs, the effect of plant ripeness remains unstudied.

Research in CQD has become increasingly focused on practical applications. Advances have been made in areas such as optoelectronics, catalysis, and sensing. Among these applications, metal ion detection has emerged as the most popular and easily achievable. Heavy metal pollutants, like copper, lead, and cadmium, are a major concern for water quality and human health worldwide. Carbon quantum dots (CQDs) offer a promising solution for the efficient detection and removal of heavy metals due to their small size, surface area, and functional groups. CQDs from natural sources, such as fruit extracts, have shown success as fluorescence sensors for heavy metal ions. Mulberry fruit-, papaya- [29], and tapioca-derived [26, 30] CQDs offer a sustainable and creative option for addressing water contamination.

Herein, we present a comprehensive study on the biosynthetic carbon quantum dots (CQDs) obtained from mulberry fruit via a hydrothermal method, focusing on their synthesis, characterization, and potential application as a highly selective sensor for Cu^{2+} ions. More importantly, the research investigates the influence of fruit ripeness on the physical and chemical properties of the obtained CQDs, which, to the best of our knowledge, has not been explored before. Extensive studies of the fluorescence properties of the obtained samples revealed different physical and chemical behaviors between CQDs obtained from ripe and unripe sources. The difference in fluorescence spectra of CQDs between ripe and unripe fruit was also observed in other fruits, such as tomatoes and blackberries. In addition, we investigated the effect of pH on the fluorescence intensity of the CQDs. Furthermore, the selective detection of Cu^{2+} ions utilizing mulberry-based CQDs with adjustable optical characteristics opens the door to the creation of highly sensitive and specific fluorescence sensors in a variety of applications. These intriguing results shed light on the relationship between fruit ripening and the emission behavior of CQDs and reveal factors such as size and molecular density changes that lead to this phenomenon.

2. Materials and Methods

2.1. Experimental Materials and Reagents. Fresh mulberries were prepared from homemade trees. Since they were all of the reagent quality, they were all used without additional purification. The deionized water was made in the chemistry laboratory.

2.2. Instrumentation and Characterization. Transmission electron microscopy (TEM) was carried out utilizing a TEM TEC9G20, FIE, USA [31]. Photoluminescence spectroscopy was performed using a homemade fluorescence spectrophotometer (tunable light source and spectrometer from SCEINCETECH 9702 (Canada)). The high-resolution X-ray diffraction (HR-XRD) was performed using a (PAN X-Pert) from the United Kingdom. Fourier transform infrared (FT-IR) spectra were taken using (Thermo-Scientific, USA). UV-Vis's absorption spectra have been recorded on a CECIL CE 7200. The 7000 series UV-Vis's measures wavelength between 190 nm and 900 nm, and an EDX instrument was used to identify the elemental composition of materials using a (QUANTA 450, Carl Zeiss Ag (supra 55VP) using an acceleration voltage of 5–30 Kv). A KT7-900-434 highspeed centrifuge was used from Heller International Trading Co., Ltd (Kenda, Germany). A DW-120D ultrasonic cleaning machine was used (Ultrasonic cleaner, China), and an AL104 electronic balance from the Mettler Toledo Instrument Co., Ltd. (Shanghai, China) was used. Finally, a high-temperature muffle furnace was taken using a DRAWELL furnace, in Shanghai, China.

2.3. Preparation of CQDs. The preparation process for synthesizing CQDs is illustrated in Figure 1. The CQDs were synthesized through a single-step solvothermal approach, employing mulberry juice as the carbon source and deionized water as the organic solvent. The procedure consists of several sequential stages. First, mulberry juice was extracted from fragmented fruit and filtered using a 0.22 μL filter. The resulting juice was centrifuged for 10 minutes at 9000 rpm to separate pulp-free mulberry juice from the supernatant. After 15 minutes, a mixture of 20 mL of filtered mulberry juice and 20 mL of deionized water was stirred. The resulting mixture is placed in a 200 mL Teflon-lined steel autoclave and heated for six hours at 180°C by the hydrothermal synthesis method [32]. After cooling the system to ambient temperature, the resulting brown products are centrifuged at 14,000 revolutions per minute for 10 minutes. The products were then subjected to freeze drying, and further testing was conducted.

2.4. Fluorescence Detection of Cu^{2+} Ions. The measurement of Cu^{2+} was conducted in a water-based solution under ambient conditions. In a standard experiment, the stock

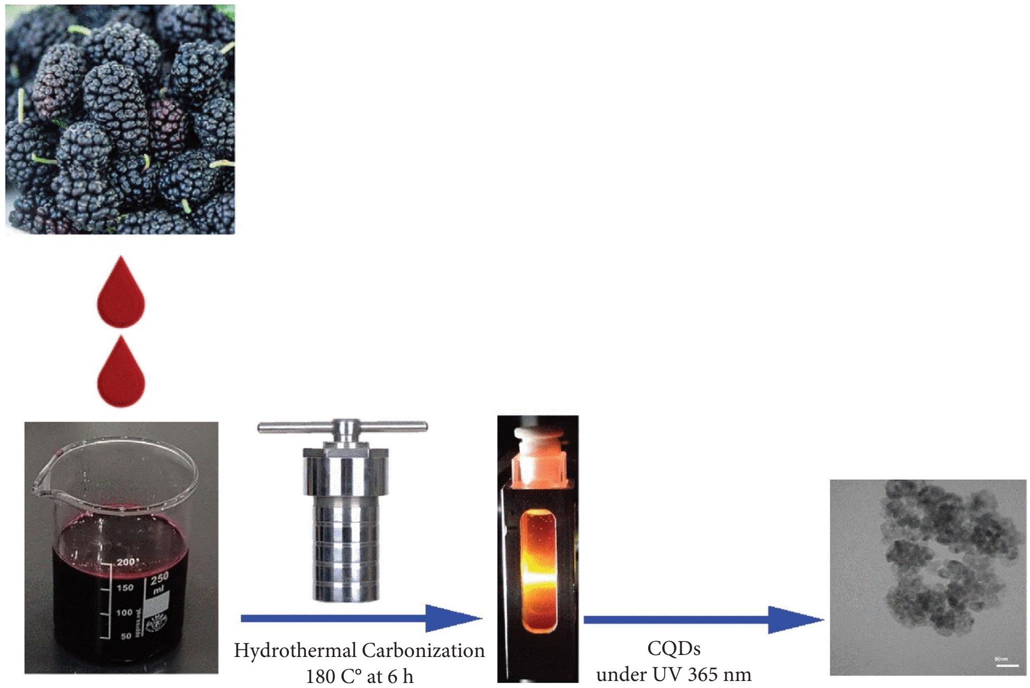

Figure 1: The preparation and procedure of CQDs from mulberry.

solutions of Cu^{2+} ions (100 mM) were generated through the process of dissolving and diluting Cu^{2+} in deionized water. To verify the presence of Cu^{2+} ions, a series of solutions with different concentrations of copper solution are mixed with a consistent volume of 1.0 mL of CQD solution. The fluorescence spectra were recorded after 2 minutes. Samples of water for the spike recovery experiment were obtained from the laboratory tap water source.

3. Results and Discussion

3.1. Structure and Morphology of CQDs. The degree of carbon ordering and crystallinity of two varieties of ripe and unripe mulberries were investigated using XRD. The XRD pattern for ripe mulberry at 180 C° is shown in Figure 2(a). The typical peak of ripe CQDs is at =21.93° which corresponds to the (002) plane with a d-spacing of 0.405 nm and can be found in the carbon material [33, 34]. The second peak is seen at 42.0498° and 49.21°, indicating the crystalline graphitic structure of the C (100) plane of the CQDs [35]. The obvious unripe CQDs' broad peak center around 20.5°, as illustrated in Figure 2(b), indicates highly disordered carbon atoms with a high degree of C (002) that still contain oxygen-containing functional groups in the CQDs. In addition, the second peaks of unripe CQDs are seen at 41.996°, 44.58°, and 48.92°, also indicating the crystalline graphitic structure of the C (100) plane of the QCDs. When comparing the ultraviolet (UV) absorption properties of ripe and unripe CQDs, a notable observation is a slight blue shift, indicating a decrease in absorption intensity. Moreover, from the results of improving the optical properties of CQDs, it has been observed that ripe CQDs exhibit greater significance compared to unripe CQDs.

The shape and size of the synthesized mulberry samples were explored by TEM. The TEM picture of ripe mulberry shows that the arranged CQDs were monodispersed and quasi-spherical with an estimated dispersion extending from 6 to 12 nm and an average diameter of 9.7 nm, as shown in Figure 3(a). The TEM picture of unripe mulberry shows that the prepared CQDs were monodispersed and quasi-spherical with dimension distribution ranging from 6 to 12 nm and a common diameter of 7.4 nm, as shown in Figure 3(b).

Energy dispersive X-ray (EDX) is a technique that reveals the presence of elements present in the materials. We use this technique to find the presence of materials in unripe and ripe mulberries. The quantity of each element that EDX found was applied, as shown in Figure 4. The EDX spectra of the synthesized ripe CQDs mostly contain carbon (72%), and oxygen (26%), and unripe CQDs mostly contain carbon (69.48) and oxygen (26%). Even after the reduction of CO, the existence of O may be caused by the presence of oxygen-containing functional groups. In addition, the presence of Au is for the coating by the gold, and Cu is the stick copper that makes it stick between the samples and the sample holder. According to the EDX spectrum, there is a larger concentration of C than O [36]. The presence of a significant concentration of oxygen elements in the adsorbent results in improved adsorption efficiency due to the strong tendency of the interfacial area to include a higher number of disrupted π–π bonds. The colloidal quantum dots (CQDs) exhibited a significant degree of oxidation due to the elevated presence of oxygen atoms, thereby leading to the formation of a greater number of reactive sites on their surface.

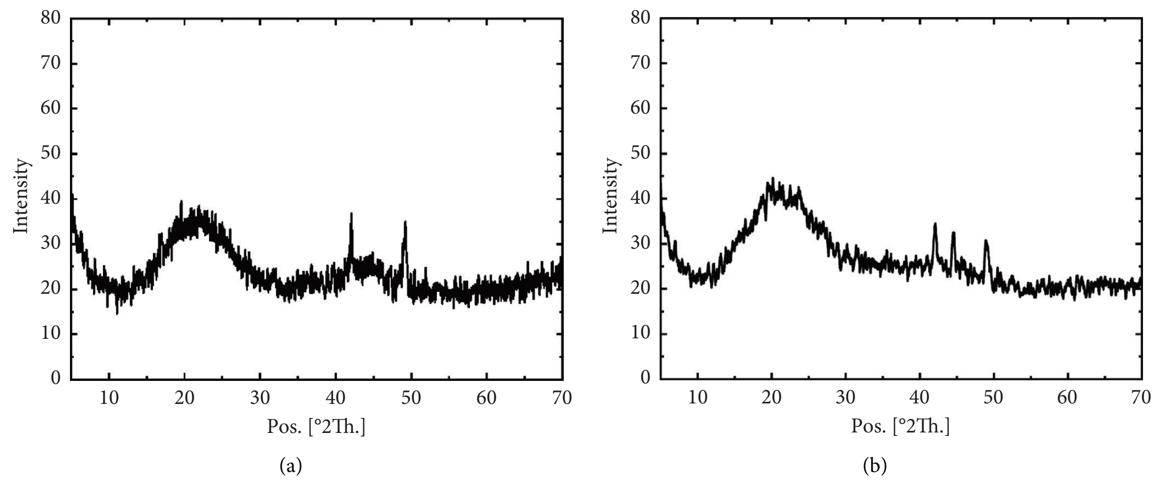

Figure 2: XRD pattern of the synthesized mulberry CQDs for (a) ripe and (b) unripe mulberry.

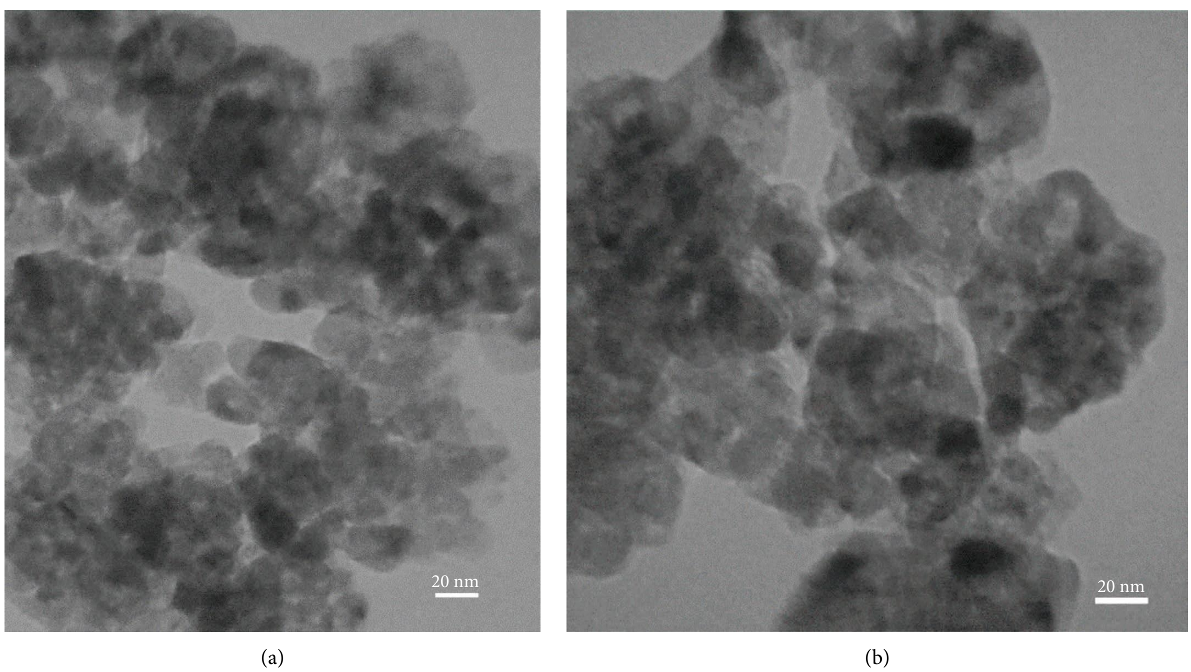

Figure 3: TEM image of the obtained CQDs for (a) ripe and (b) unripe mulberry.

3.2. Surface Chemistry Composition Analysis. FT-IR spectroscopy was used to examine the chemical structure and makeup of CQDs, as illustrated in Figure 5. For the pure ripe and unripe mulberry powder, the clear broad peaks at 3236 cm^{-1} ripe mulberry and 3294 cm^{-1} unripe mulberries correspond to the O-H stretching vibration and the absorption bands at 2885 cm^{-1} and 2098 cm^{-1} had been attributed to the C=C stretching vibration [1, 37]. The absorption band at 1631 cm^{-1} for both types of mulberries was identified as the C=O bending vibration. The peaks at 1192 cm^{-1} and 1519 cm^{-1} were due to the C=C stretching vibrations. The peaks at 976 cm^{-1} and 980 cm^{-1} were attributed to the vibrations of C-H bonds. The peaks at 671 cm^{-1} and 663 cm^{-1} were due to C-H bonds, respectively. Compared to mulberry, CQDs showed an obvious minimization in the absorption of O-H stretching vibrations at 3236 cm^{-1} for ripe mulberry and 3294 cm^{-1} for unripe mulberry, and C-H vibrations at 671 cm^{-1} for ripe mulberry and 663 cm^{-1} for unripe mulberry. Moreover, the three clear absorption peaks at 3236, 1631, and 671 cm^{-1} are related to the stretching and bending vibrations of O-H, C=C, and C-H, respectively. FT-IR analysis validated the existence of hydroxyl and carbonyl functionalities on the surface of CQDs.

3.3. Optical Properties of CQDs. The most useful method for examining the optical properties of CQDs is UV-vis spectroscopy. The UV-Vis spectrum of the CQDs was found to have one characteristic absorption peak located at wavelengths of 243 nm for ripe CQDs and a second peak located around 282 nm for unripe CQDs in the spectrum as

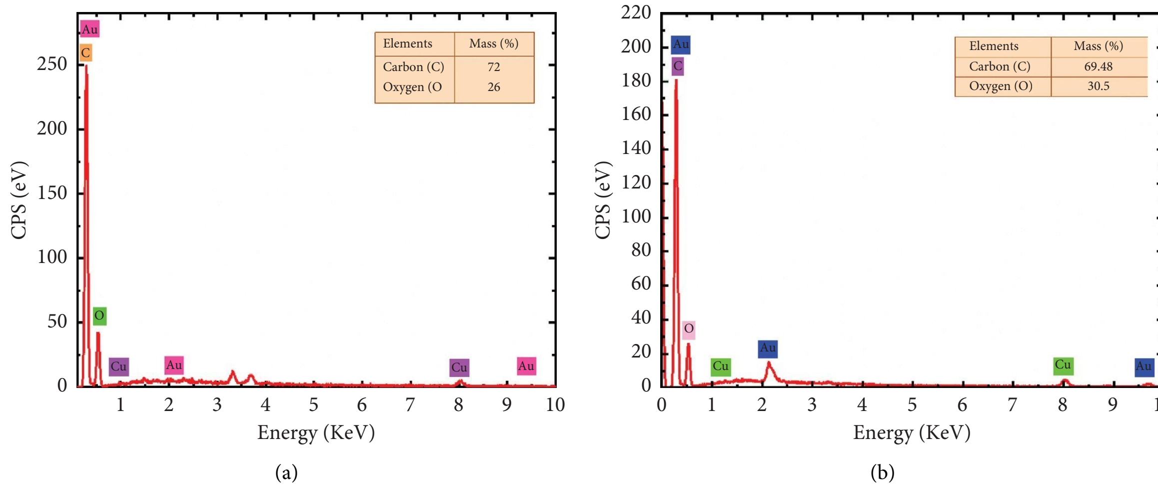

Figure 4: EDX spectrum of the prepared CQDs. (a) Ripe mulberry. (b) Unripe mulberry.

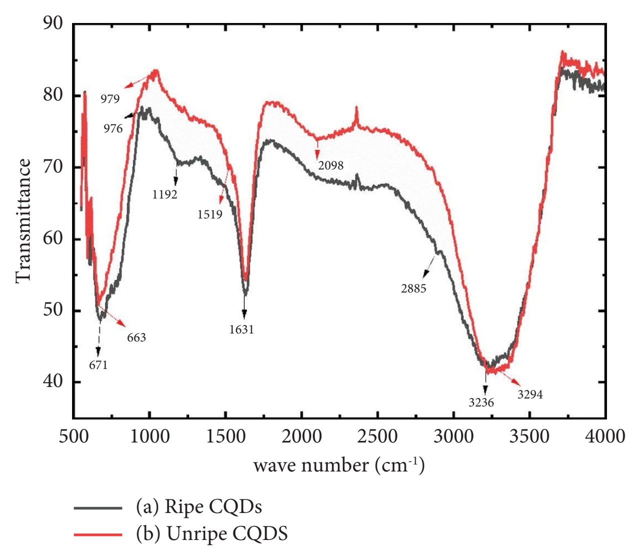

Figure 5: (a) FTIR spectra of prepared CQDs from ripe mulberry. (b) FTIR spectra of prepared CQDs from unripe mulberry.

illustrated in Figure 6. These peaks are associated with a π–π^* transition of aromatic -C=C- bonds aromatic sp^2 hybridization and n–π^* transition of the conjugated C=O band which is similar to early reports [36, 38, 39]. The progressive increase in unripe CQDs results in a shift towards longer wavelengths in the absorption, indicating the occurrence of ground-state complex formation in CQD.

The PL emission spectra properties of the CQDs were investigated. It is well known that the PL emission intensity of the CQDs is highly dependent on the excitation wavelengths [40, 41]. Figure 7 presents the feature of excitation-dependent emission spectra showing different maximum emission wavelengths under the variation of the excitation wavelength changing from 350 to 450 nm for the ripe and unripe mulberry. The CQDs excited at 400 nm show strong yellow PL located at 500 nm for unripe mulberry and 510 nm for ripe mulberry; this behavior is frequently observed in some carbon dots and can be attributed to different emissive states present on the surface of carbon dots. When the excitation wavelength was changed from 350 to 450 nm, the PL intensity gradually increased due to the graphitic carbon cores of the CQDs transitioning from π to π^*, and the PL emission peaks were significantly red-shifted, as shown in Figures 7(a) and 7(b). The result reveals that CQDs show different optical properties based on their ripeness. This may be anticipated to be caused by variations in their molecular densities and other chemical characteristics, such as functional groups [42, 43].

To understand the role of ripe and unripe plants on their optical properties and to find whether the ripeness effect on optical properties may only occur in mulberry fruit, PL spectra from other two green sources (tomatoes and blackberries) were tested, as displayed in Figure 8. The PL properties of both green source materials showed a similar

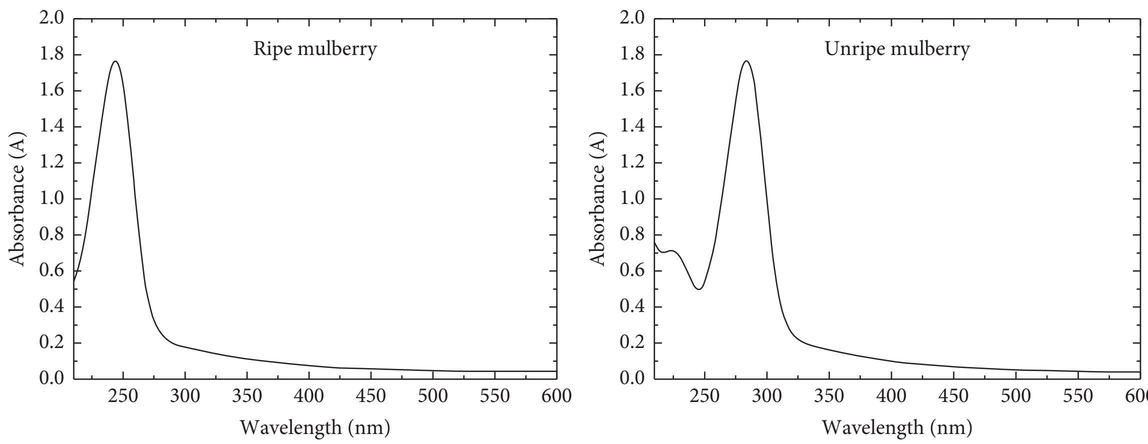

Figure 6: UV-visible absorption spectra of ripe and unripe mulberries.

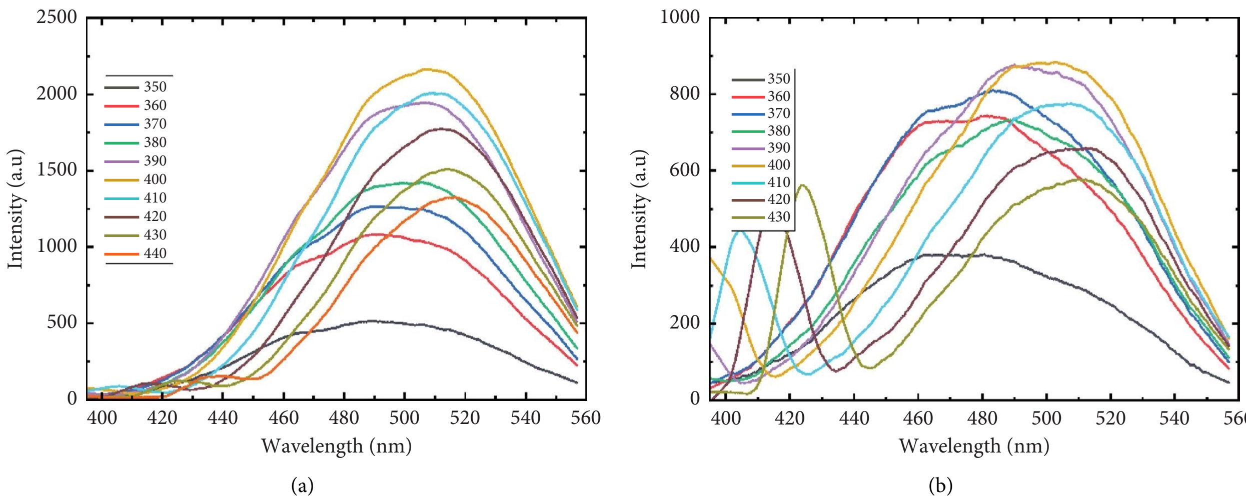

Figure 7: Excitation light-dependent PL emission spectrum of CQDs for the (a) ripe mulberry and (b) unripe mulberry.

trend as the mulberry fruit and as expected exhibited excellent excitation light-dependent photoluminescence (PL) emissions. However, interestingly, the PL spectra of the unripe and ripe parts of both plants exhibited a notable shift. The results showed that the maximum PL spectra of the ripe tomato CQDs (Figure 8(a)) were located at 503 nm under a 410 nm wavelength excitation, while the maximum PL spectra of the unripe tomato CQDs (Figure 8(b)) was at 490 nm under a 400 nm wavelength excitation. A similar trend of emission properties was found for the blackberry CQDs, and the results showed maximum PL spectra of the ripe blackberry CQDs (Figure 8(c)) at 523 nm under a 490 nm wavelength, while the maximum PL spectra of the unripe blackberry CQDs (Figure 8(d)) were located at 492 nm under a 400 nm wavelength. This result specified that the plant's ripeness indeed slightly modulates its optical properties. This could be due to the different sizes of the CQDs for ripe and unripe fruit [27].

4. Detection of Cu^{2+}

The sensing characteristics of CQD detection systems are critically dependent on selectivity. To validate the selectivity of the CQDs to Cu^{2+} ions, the fluorescence intensity of CQDs solutions in the presence of various metal ions (Ag^+, Fe^{3+}, Zn^{2+}, Pb^{2+}, Cd^{2+}, Co^{2+}, Na^+, K^+, Hg^{2+}, Cu^{2+}, Cl^-, SO_4^{2-}, and NO_3^-) was explored. The fluorescence response of the CQDs solution towards various metal ions each at a consistent concentration of 100 mM was recorded at an excitation wavelength of 370 nm. Figure 9 displays the behaviors of the fluorescence quenching of the various metal ions. Cu^{2+} ions addition showed a remarkable effect on the CQDs fluorescence response compared to other metal ions that showed a negligible effect on fluorescence intensity. These results revealed that the prepared CQDs could be successfully used to selectively detect Cu^{2+} ions by recording the fluorescence intensity. Cu^{2+} ions can specifically

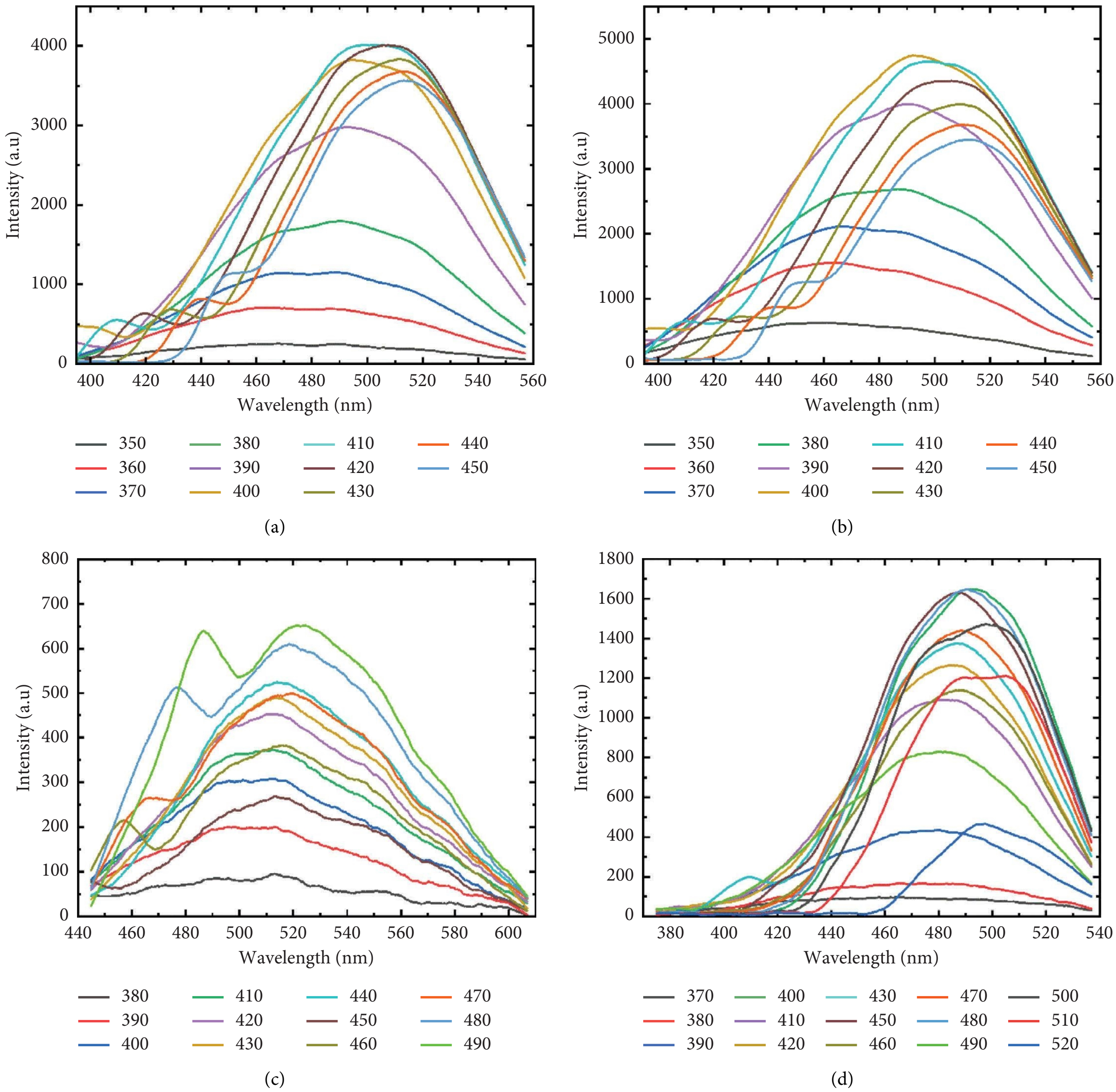

Figure 8: The CQDs' fluorescence spectra at various excitation wavelengths. (a) The PL of the ripe tomato at 180 C°. (b) The PL of the unripe tomato at 180 C°. (c) The PL of the ripe blackberry at 180 C° and (d) the PL of the unripe blackberry at 180 C°.

coordinate with the phenolic hydroxyl groups on the surface of CQDs to quench their fluorescence [44–46].

The effective energy transfer between Cu^{2+} and the groups on the surface of the CQDs may be the cause of the fast fluorescence quenching, as shown in Figure 10.

It becomes clear that CQDs can be used as a sensitive fluorescence sensor for Cu^{2+} ion detection (Table 1). The sensitivity of the prepared CQDs for the determination of Cu^{2+} ions was also investigated. As the concentration of Cu^{2+} ions increased, the fluorescence intensity of the carbon quantum dots CQDs was observed to gradually decrease, as depicted in Figure 11. Consequently, the ratio of the fluorescence intensity (I) to the initial fluorescence intensity (I_0), denoted as I/I_0, decreased linearly with the concentration of Cu^{+2} ions in the range 0.1 to 1 μM, displaying a strong linear correlation with a coefficient of determination (R^2) of 0.9864, as illustrated in Figure 11. The detection limit was 0.2687 μM, and the limit of qualification (LOQ) is 0.814 μM, indicating that the CQDs pose potential utility to be used as a fluorescence sensor for Cu^{2+} ions detection [45].

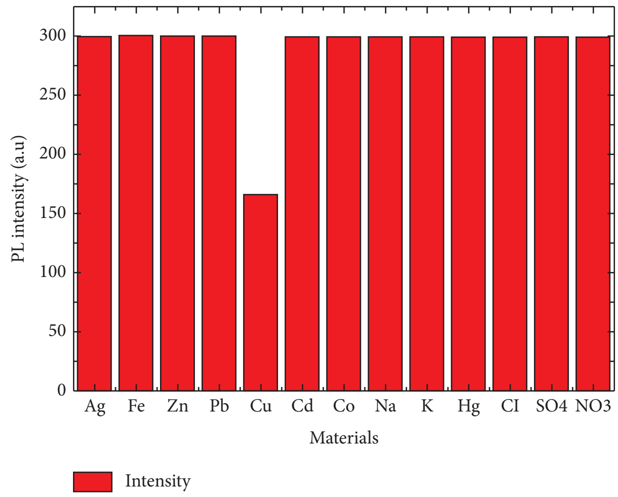

FIGURE 9: The impact of various ions on the fluorescence of carbon quantum dots (CQDs).

FIGURE 10: The recorded fluorescence images of a CQD solution before (left) and after (right) Cu^{2+} ion addition at room temperature.

TABLE 1: A summary of Cu^{2+} sensors based on CQDs.

CQDs sensors	Detection limits	Ranges	Reference
Ionic liquid-derived CQDs	0.18 μM	0.5–5 μM and 10–90 μM	[47]
CQDs from sago waste	7.78 μM	0–47 μM	[48]
CdSe/ZnS@CQDs	1 μM	1–100 μM	[49]
CQDs from citric acid	0.63 μM	0.37–2.5 μM	[50]
Silica-coated CQDs	0.3 μM	0.833–833 μM	[51]
Agarose/CQDs	0.5 μM	—	[52]
N-CQDs	0.09 μM/0.12 μM	0.3–1.6 μM	[53]

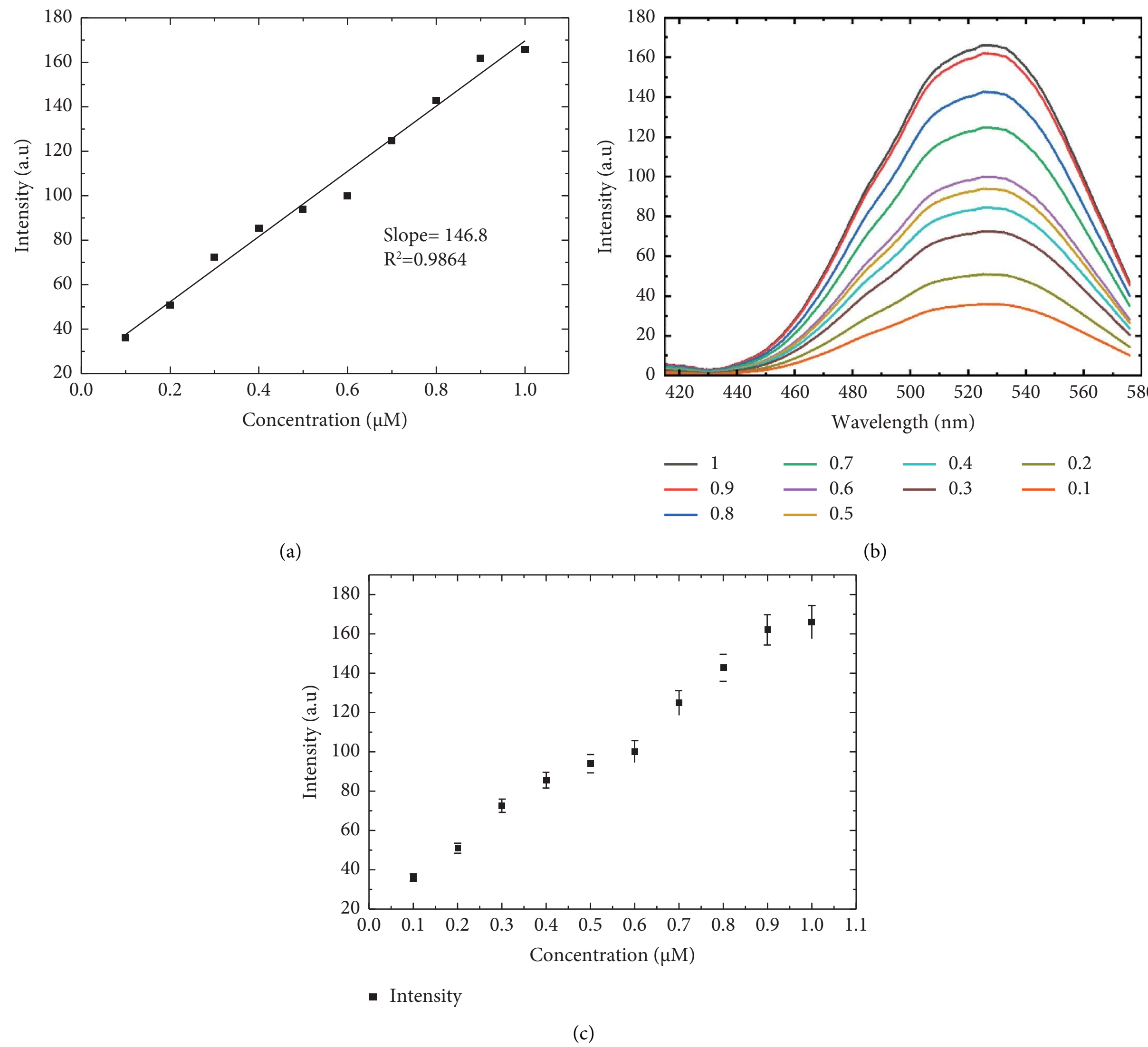

Figure 11: (a) The intensity of CQD with the concentration of Cu^{2+} ions, (b) the PL intensity of CQDs with Cu^{2+} in different concentrations, and (c) the error bar of CQDs with Cu^{2+} in different concentrations.

5. Conclusion

This study successfully created green luminescent carbon quantum dots (CQDs) through a simple hydrothermal method, using mulberry fruit as the carbon source. The physical and chemical properties of the CQDs were investigated, revealing that fruit ripeness directly impacted the fluorescence spectra and characteristics of the CQDs. The fluorescence spectra and high-resolution transmission electron microscopy (HR-TEM) images showed that the average diameter and intensity of photoluminescence (PL) of CQDs changed depending on how ripe the fruit was. Under 400 nm excitation, the PL peak was 510 nm for ripe and 500 nm for unripe mulberries, with corresponding CQD sizes of 9.7 and 7.4 nm, respectively. The CQDs also showed excitation-dependent PL emissions due to surface state defects. Energy-dispersive X-rays (EDX) and X-ray diffraction (XRD) showed that the CQDs made in the laboratory were graphitic and had hydroxyl and carboxyl groups on the surface. These groups are mostly made of carbon and oxygen. Fourier-transform infrared (FT-IR) analysis revealed that the surface functional groups consisted of O-H, C=O, and C=C functional groups. The synthesized CQDs demonstrated exceptional selectivity and sensitivity towards Cu^{+2} ions, with a detection limit (DL) of 0.2687 μM and a limit of qualification (LOQ) of 0.814 μM. A strong linear relationship between Cu^{2+} ion fluorescence intensity and concentrations within the 0.1–1 μM range was established through fluorescence quenching, demonstrating its capacity for sensitive Cu^{2+} ion detection. These CQDs are a promising solution for fluorescence-based detection applications because of their easy and cost-effective synthesis.

Data Availability

All underlying data are available as part of the article and no additional source data are required.

Conflicts of Interest

The authors declare that they have no conflicts of interest.

Authors' Contributions

Chiayee Salih Ajaj investigated (equal) the study, designed a methodology (equal), and wrote, reviewed, and edited (equal) the manuscript. Diyar Sadiq designed a methodology (equal), supervised the study (equal), and wrote, reviewed, and edited (equal) the manuscript.

Acknowledgments

The authors would like to thank Mr Shinwar A. Idrees for his support.

References

[1] S. Borna, R. E. Sabzi, and S. Pirsa, "Synthesis of carbon quantum dots from apple juice and graphite: investigation of fluorescence and structural properties and use as an electrochemical sensor for measuring Letrozole," *Journal of Materials Science: Materials in Electronics*, vol. 32, no. 8, pp. 10866–10879, 2021.

[2] S. Kang, H. Han, K. Lee, and K. M. Kim, "Ultrasensitive detection of Fe3+Ions using functionalized graphene quantum dots fabricated by a one-step pulsed laser ablation process," *ACS Omega*, vol. 7, no. 2, pp. 2074–2081, 2022.

[3] P. Das, "Green approach to photoluminescent carbon dots for imaging of gram-negative bacteria *Escherichia coli*," *Nanotechnology*, vol. 28, pp. 195501–195519, 2017.

[4] A. Saravanan, "Applications of N-doped carbon dots as antimicrobial agents, antibiotic carriers, and selective fluorescent probes for nitro explosives," *ACS Applied Bio Materials*, vol. 3, no. 11, pp. 8023–8031, 2020.

[5] P. Das, "Carbon dots for heavy-metal sensing, pH-sensitive cargo delivery, and antibacterial applications," *ACS Applied Nano Materials*, vol. 3, no. 12, pp. 11777–11790, 2020.

[6] T. Feng, X. Ai, G. An, P. Yang, and Y. Zhao, "Charge-convertible carbon dots for imaging-guided drug delivery with enhanced in vivo cancer therapeutic efficiency," *ACS Nano*, vol. 10, no. 4, pp. 4410–4420, 2016.

[7] V. C. Hoang, K. Dave, and V. G. Gomes, "Carbon quantum dot-based composites for energy storage and electrocatalysis: mechanism, applications and future prospects," *Nano Energy*, vol. 66, Article ID 104093, 2019.

[8] S. N. Baker and G. A. Baker, "Luminescent carbon nanodots: emergent nanolights," *Angewandte Chemie International Edition*, vol. 49, no. 38, pp. 6726–6744, 2010.

[9] P. Das, S. Ganguly, S. Banerjee, and N. C. Das, "Graphene Based Emergent Nanolights: A Short Review on the Synthesis, properties and application," *Research on Chemical Intermediates*, vol. 45, no. 7, 2019.

[10] X. Zhang, "Color-switchable electroluminescence of carbon dot light-emitting diodes," *ACS Nano*, vol. 7, no. 12, pp. 11234–11241, 2013.

[11] S. Liu, "Hydrothermal treatment of grass: a low-cost, green route to nitrogen-doped, carbon-rich, photoluminescent polymer nanodots as an effective fluorescent sensing platform for label-free detection of Cu(II) ions," *Advanced Materials*, vol. 24, no. 15, pp. 2037–2041, 2012.

[12] M. J. Molaei, "The optical properties and solar energy conversion applications of carbon quantum dots: a review," *Solar Energy*, vol. 196, pp. 549–566, 2020.

[13] A. Saravanan, M. Maruthapandi, P. Das, J. H. T. Luong, and A. Gedanken, "Green synthesis of multifunctional carbon dots with antibacterial activities," *Nanomaterials*, vol. 11, no. 2, pp. 1–11, 2021.

[14] W. K. Li, J. T. Feng, and Z. Q. Ma, "Nitrogen, sulfur, boron and flavonoid moiety co-incorporated carbon dots for sensitive fluorescence detection of pesticides," *Carbon*, vol. 161, pp. 685–693, 2020.

[15] V. Arul and M. G. Sethuraman, "Facile green synthesis of fluorescent N-doped carbon dots from Actinidia deliciosa and their catalytic activity and cytotoxicity applications," *Optical Materials*, vol. 78, pp. 181–190, 2018.

[16] S. Wu, C. Zhou, C. Ma, Y. Yin, and C. Sun, "Carbon quantum dots-based fluorescent hydrogel hybrid platform for sensitive detection of iron ions," *Journal of Chemistry*, vol. 2022, Article ID 3737646, 14 pages, 2022.

[17] X. Huo, "Green synthesis of carbon dots from grapefruit and its fluorescence enhancement," *Journal of Nanomaterials*, vol. 2020, Article ID 8601307, 7 pages, 2020.

[18] H. Zhang, J. You, J. Wang, X. Dong, R. Guan, and D. Cao, "Highly luminescent carbon dots as temperature sensors and 'off-on' sensing of Hg2+ and biothiols," *Dyes and Pigments*, vol. 173, Article ID 107950, 2020.

[19] X. Wang, K. Qu, B. Xu, J. Ren, and X. Qu, "Microwave assisted one-step green synthesis of cell-permeable multicolor photoluminescent carbon dots without surface passivation reagents," *Journal of Materials Chemistry*, vol. 21, no. 8, pp. 2445–2450, 2011.

[20] S. K. Bhunia, A. Saha, A. R. Maity, S. C. Ray, and N. R. Jana, "Carbon nanoparticle-based fluorescent bioimaging probes," *Scientific Reports*, vol. 3, no. 1, p. 1473, 2013.

[21] I. Alkian, H. Sutanto, B. Hadiyanto, A. Prasetio, and B. Aprimanti Utami, "Facile synthesized carbon dots for simple and selective detection of cobalt ions in aqueous media," *Cogent Engineering*, vol. 9, no. 1, 2022.

[22] B. S. B. Kasibabu, S. L. D'Souza, S. Jha, and S. K. Kailasa, "Imaging of bacterial and fungal cells using fluorescent carbon dots prepared from Carica papaya juice," *Journal of Fluorescence*, vol. 25, no. 4, pp. 803–810, 2015.

[23] Z. Lai, X. Guo, Z. Cheng, G. Ruan, and F. Du, "Green synthesis of fluorescent carbon dots from cherry tomatoes for highly effective detection of trifluralin herbicide in soil samples," *ChemistrySelect*, vol. 5, no. 6, pp. 1956–1960, 2020.

[24] C. Dias, "Biocompatibility and bioimaging potential of fruit-based carbon dots," *Nanomaterials*, vol. 9, no. 2, p. 199, 2019.

[25] M. Y. Pudza, Z. Z. Abidin, S. Abdul-Rashid, F. M. Yassin, A. S. M. Noor, and M. Abdullah, "Synthesis and characterization of fluorescent carbon dots from tapioca," *ChemistrySelect*, vol. 4, no. 14, pp. 4140–4146, 2019.

[26] M. Y. Pudza, Z. Z. Abidin, S. Abdul-Rashid, F. M. Yasin, A. S. M. Noor, and J. Abdullah, "Selective and simultaneous detection of cadmium, lead and copper by tapioca-derived carbon dot–modified electrode," *Environmental Science & Pollution Research*, vol. 27, no. 12, pp. 13315–13324, 2020.

[27] B. T. Hoan, P. D. Tam, and V. H. Pham, "Green synthesis of highly luminescent carbon quantum dots from lemon juice,"

Journal of Nanotechnology, vol. 2019, Article ID 2852816, 9 pages, 2019.

[28] M. He, J. Zhang, H. Wang, Y. Kong, Y. Xiao, and W. Xu, "Material and optical properties of fluorescent carbon quantum dots fabricated from lemon juice via hydrothermal reaction," *Nanoscale Research Letters*, vol. 13, no. 1, p. 175, 2018.

[29] K. K. Gudimella, "Novel synthesis of fluorescent carbon dots from bio-based Carica Papaya Leaves: optical and structural properties with antioxidant and anti-inflammatory activities," *Environmental Research*, vol. 204, Article ID 111854, 2022.

[30] M. Y. Pudza, Z. Z. Abidin, S. A. Rashid, F. M. Yasin, A. S. M. Noor, and M. A. Issa, "Eco-friendly sustainable fluorescent carbon dots for the adsorption of heavy metal ions in aqueous environment," *Nanomaterials*, vol. 10, no. 2, pp. 1–19, 2020.

[31] Q. Zhang, "The application of green-synthesis-derived carbon quantum dots to bioimaging and the analysis of mercury(II)," *Journal of Analytical Methods in Chemistry*, vol. 2019, Article ID 8183134, 9 pages, 2019.

[32] M. Y. Pudza, Z. Z. Abidin, S. A. Rashid, F. M. Yasin, A. S. M. Noor, and M. A. Issa, "Sustainable synthesis processes for carbon dots through response surface methodology and artificial neural network," *Processes*, vol. 7, p. 10, 2019.

[33] V. Arul and M. G. Sethuraman, "Hydrothermally green synthesized nitrogen-doped carbon dots from Phyllanthus emblica and their catalytic ability in the detoxification of textile effluents," *ACS Omega*, vol. 4, no. 2, pp. 3449–3457, 2019.

[34] C. Zhou, S. Wu, S. Qi, W. Song, and C. Sun, "Facile and high-yield synthesis of N-doped carbon quantum dots from biomass quinoa saponin for the detection of Co2+," *Journal of Analytical Methods in Chemistry*, vol. 2021, Article ID 9732364, 11 pages, 2021.

[35] Y. Yan, S. Manickam, E. Lester, T. Wu, and C. H. Pang, "Synthesis of graphene oxide and graphene quantum dots from miscanthus via ultrasound-assisted mechano-chemical cracking method," *Ultrasonics Sonochemistry*, vol. 73, Article ID 105519, 2021.

[36] T. Selvakumar, M. Rajaram, A. Natarajan, L. Harikrishnan, K. Alwar, and A. Rajaram, "Highly efficient sulfur and nitrogen Co-doped graphene quantum dots as a metal-free green photocatalyst for photocatalysis and fluorescent ink applications," *ACS Omega*, vol. 7, no. 15, pp. 12825–12834, 2022.

[37] A. Kurdekar, L. A. A. Chunduri, E. P. Bulagonda, M. K. Haleyurgirisetty, V. Kamisetti, and I. K. Hewlett, "Comparative performance evaluation of carbon dot-based paper immunoassay on Whatman filter paper and nitrocellulose paper in the detection of HIV infection," *Microfluidics and Nanofluidics*, vol. 20, no. 7, p. 99, 2016.

[38] K. Jlassi, K. Eid, M. H. Sliem, A. M. Abdullah, M. M. Chehimi, and I. Krupa, "Rational synthesis, characterization, and application of environmentally friendly (polymer–carbon dot) hybrid composite film for fast and efficient UV-assisted Cd2+ removal from water," *Environmental Sciences Europe*, vol. 32, no. 1, p. 12, 2020.

[39] F. Lu, "Highly fluorescent nitrogen-doped graphene quantum dots' synthesis and their applications as Fe(III) ions sensor," *International Journal of Optics*, vol. 2019, Article ID 8724320, 9 pages, 2019.

[40] Y. Coşkun, "Development of highly luminescent water-insoluble carbon dots by using calix[4]pyrrole as the carbon precursor and their potential application in organic solar cells," *ACS Omega*, vol. 7, no. 22, pp. 18840–18851, 2022.

[41] Q. Huang, Z. Y. Zhou, and Q. Lv, "Room-temperature synthesized carbon quantum dots and potential applications to cell imaging," *Digest Journal of Nanomaterials and Biostructures*, vol. 18, no. 1, pp. 195–202, 2023.

[42] H. Lin, J. Huang, and L. Ding, "Preparation of carbon dots with high-fluorescence quantum yield and their application in dopamine fluorescence probe and cellular imaging," *Journal of Nanomaterials*, vol. 2019, Article ID 5037243, 9 pages, 2019.

[43] Y. J. Sun, J. S. Tang, L. Xiang, X. Hu, J. Wei, and X. J. Song, "Hydrothermal synthesis of high-performance nitrogen-doped carbon quantum dots from Ophiopogon japonicus and their application in sensing Fe (III) with a broad quantitative range," *Digest Journal of Nanomaterials and Biostructures*, vol. 17, no. 4, pp. 1327–1343, 2022.

[44] X. Gao, C. Du, Z. Zhuang, and W. Chen, "Carbon quantum dot-based nanoprobes for metal ion detection," *Journal of Materials Chemistry C: Materials for Optical and Electronic Devices*, vol. 4, no. 29, pp. 6927–6945, 2016.

[45] J. Yang, Z. Guo, and X. Yue, "Preparation of carbon quantum dots from corn straw and their application in Cu2+ detection," *Bioresources*, vol. 17, no. 1, pp. 604–615, 2021.

[46] H. Qi, "Biomass-derived nitrogen-doped carbon quantum dots: highly selective fluorescent probe for detecting Fe 3+ ions and tetracyclines," *Journal of Colloid and Interface Science*, vol. 539, pp. 332–341, 2019.

[47] P. Xu, C. Wang, D. Sun, Y. Chen, and K. Zhuo, "Ionic liquid as a precursor to synthesize nitrogen- and sulfur-co-doped carbon dots for detection of copper(II) ions," *Chemical Research in Chinese Universities*, vol. 31, no. 5, pp. 730–735, 2015.

[48] X. W. Tan, A. N. B. Romainor, S. F. Chin, and S. M. Ng, "Carbon dots production via pyrolysis of sago waste as potential probe for metal ions sensing," *Journal of Analytical and Applied Pyrolysis*, vol. 105, pp. 157–165, 2014.

[49] A. Zhu, Q. Qu, X. Shao, B. Kong, and Y. Tian, "Carbon-dot-based dual-emission nanohybrid produces a ratiometric fluorescent sensor for in vivo imaging of cellular copper ions," *Angewandte Chemie International Edition*, vol. 51, no. 29, pp. 7185–7189, 2012.

[50] A. Salinas-Castillo, "Evaluation of a reconfigurable portable instrument for copper determination based on luminescent carbon dots," *Analytical and Bioanalytical Chemistry*, vol. 408, no. 11, pp. 3013–3020, 2016.

[51] Y. Lin, "Tunable fluorescent silica-coated carbon dots: a synergistic effect for enhancing the fluorescence sensing of extracellular Cu2+ in rat brain," *ACS Applied Materials and Interfaces*, vol. 7, no. 49, pp. 27262–27270, 2015.

[52] N. Gogoi, M. Barooah, G. Majumdar, and D. Chowdhury, "Carbon dots rooted agarose hydrogel hybrid platform for optical detection and separation of heavy metal ions," *ACS Applied Materials and Interfaces*, vol. 7, no. 5, pp. 3058–3067, 2015.

[53] A. Salinas-Castillo, "Carbon dots for copper detection with down and upconversion fluorescent properties as excitation sources," *Chemical Communications*, vol. 49, no. 11, pp. 1103–1105, 2013.